

INVESTIGATION ON THE VARIATION OF THE TENSION AXIAL STIFFNESS OF COLUMNS AND PANELS IN ASEISMIC HIGH-STRENGTH RC WALLS

H. Ousalem¹ and H. Kimura²

¹ *Researcher, Takenaka Research & development Institute, Chiba, Japan*

² *Senior Chief Researcher, Takenaka Research & development Institute, Chiba, Japan*
Email: ousalem.hassane@takenaka.co.jp, hideki.kimura@takenaka.co.jp

ABSTRACT :

Predicting inelastic responses of reinforced concrete walls requires well-defined and effective modeling besides the analysis platform tool. Such modeling can be accomplished by using microscopic or macroscopic models. Therefore due to various complexities involved in the former models, the later models are more effective due to relatively simple implementation and reasonably accurate in predicting the response of RC walls. This study discusses the tension axial stiffness ratio proposed in an existing procedure (Kabeyasawa macro-model for shear walls), which is widely used by researchers and design practicing engineers for modeling reinforced concrete walls. The feasibility of a different application of the original model was checked through pushover analyses and test data. Test data of wall specimens with boundary columns and wall specimens with rectangular sections were used. The examination procedure was based on two parameters: the variation of the number of panels constituting a given wall and the simultaneous variation of the tension axial stiffness ratio of both panels and columns along the wall-height. From the results of several simulations on different modeling and their matching to test results, suitable varying values of the tension stiffness ratio were selected according to the number of panels. They are presented and suggested for a better assessment of structural wall seismic response.

KEYWORDS: RC walls, Wall of rectangular shape, Wall with boundary columns, Kabeyasawa model, Tension axial stiffness ratio, High-strength materials

1. INTRODUCTION

As stated in different investigation reports (AIJ, 2001; Ousalem, 2003; Bechtoula, 2005), in most cases, buildings with structural walls resisted effectively lateral loads imposed by earthquakes. Such structural elements, when properly designed and constructed, provide substantial strength and stiffness as well as the deformation capacity needed to meet the demands of strong motions. To respond adequately to such hazard, predicting inelastic responses of reinforced concrete walls requires well-defined and effective modeling besides the analysis platform tool. Such modeling can be accomplished by using microscopic (finite element) or macroscopic models. Although micro-models can provide a refined and detailed definition of the local response, their efficiency and practicality are questionable due to the complexities involved in at different stages, particularly, interpreting the results when the size of the structure becomes large. For such reason, macro-models are more effective for analysis and design by their relatively simple implementation, are reasonably accurate in predicting the response of RC walls and not complicated when interpreting the results. The structural modeling based on non-linear force-displacement (non-linear moment-rotation) relations of individual structural members is the most common where various member models as well as a large number of hysteresis models have been proposed and investigated (Takeda, 1970; Kabeyasawa, 1983; Kangning, 1988; Kangning, 1993) based on experimental studies of destructive

tests of scaled and of actual size structural members and their assemblies. Among existing models, Kabeyasawa model (Kabeyasawa, 1983), which is widely used by researchers and design practicing engineers for modeling reinforced concrete walls, is assumed composed of a central panel and two columns at the edges of the panel. All consist of non-linear springs that connect the top and bottom rigid beams (rigid floors). As illustrated in Fig. 1, the main wall (panel) is represented by three sub-elements (a shear spring, an axial spring and a bending spring at the base) while the boundary-column elements are assumed with hinges at their ends and represented by an axial spring each where the tension stiffness K_t is originally considered 90% (tension axial stiffness ratio ϕ value proposed by Kabayasawa) of the compression stiffness K_c . The wall behavior is considerably controlled by the axial springs and their modeling is of importance. This macro-model was pointed in a different study (Vulcano, 1986) as the most suitable for incorporation in the non-linear analysis of multi-story frame-wall structural systems. However, the same study reported that the response was not adequately described for dominated shear stresses. Since then, this model has been developed to overcome the previous mentioned insufficiency but it lacked, in some studies (Kabeyasawa, 1997), its previous simplicity.

In this study, the change in wall response was investigated through simultaneous settings of the axial tension stiffness ratio along the height of the boundary columns and the central panel, and also the increase in the number of panels forming the wall. The feasibility of this different application of the original model was checked through pushover analyses and test data. In order to widen the conclusions, test data of wall specimens with boundary columns and wall specimens of rectangular cross-sections were used. From the results of several simulations on different modeling and their matching to test results, suitable varying values of the tension stiffness ratio were selected according to the number of panels. They are presented and suggested for a better assessment of structural wall seismic response.

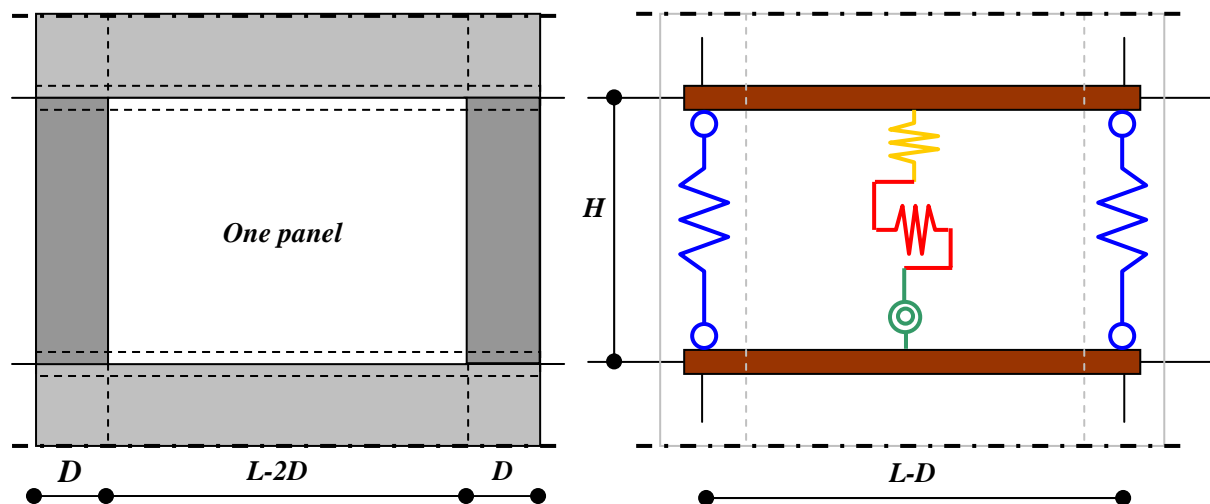


Figure 1 Wall elevation scheme and assumed Kabeyasawa model for one panel

2. TEST DATA AND ANALYZED SPECIMENS

The analysis was performed for five wall-specimens tested previously (Kimura, 2006; Takenaka, 2003), three of them were of rectangular cross section, referenced C07N10, C07N15 and C10N10, and the other two were with boundary columns, referenced C2 and D1. The specimens were made with high-strength materials as presented in Table 1. A certain amount of reinforcement was concentrated at the vertical boundary edges/columns of the walls and another appropriate amount was distributed on the web/panel. The main details of the specimens are shown in Fig. 2 through Fig. 4.

Table 1 Main characteristics of wall-specimens

	Wall	C07N10		C07N15		C10N10		C2		D1	
		C	P	C	P	C	P	C	P	C	P
Longitudinal reinforcement	ρ_g (%)	3.95	0.95	3.95	0.95	3.95	0.95	2.13	1.17	3.81	1.16
	f_y (MPa)	718	802	718	802	718	802	393	865	367	421
Transverse reinforcement	ρ_w (%)	1.97	0.95	1.97	0.95	1.97	0.95	1.13	1.17	0.90	1.16
	f_y (MPa)	767	802	767	802	767	802	868	865	942	421
Cross-section	A (cm ²)	450*	1350	450*	1350	450*	1350	400*	800	400*	1275
Columns/panel section ratio	(%)	66.67**		66.67**		66.67**		100**		62.75**	
Concrete strength	f_c (MPa)	74.9		74.9		109.1		79.0		63.0	
Axial Load	N (kN)	1700		2500		2500		1250		1350	
Axial load ratio	η	0.10		0.15		0.10		0.13		0.11	
Shear-span ratio	a	2.00		2.00		2.00		2.00		1.80	

Notes: C= Column, P= Panel, * = cross-section of one column, ** = two columns' sections considered

3. MODELING AND PARAMETERS

The pushover analysis was carried out to simulate the response of the wall to a monotonic loading by investigating the influence of the following parameters:

1. The tension axial stiffness ratio ϕ of columns and panels, and
2. The number of panel layers forming the wall.

At first, the analysis was performed for one panel-layer wall (Fig.1) considering extreme cases ($\phi=0.9$ and $\phi=0.1$) for all vertical sub-elements in order to find out the range of influence brought by each case. The value $\phi=0.9$ was the value suggested in the original model by Professor Kabeyasawa, while the value $\phi=0.1$ was taken as a half of the average value computed considering only the effect of the longitudinal reinforcement section in the columns of the tested specimens. The computed average value was equal to $\phi=0.2$.

As a second step, other analyses were carried out considering two and three-panel-layer cases (Fig.5) with variable tension axial stiffness ratios. Different trials were carried out for each case in order to match the test data. Besides varying the number of panels, varying the tension axial stiffness ratio of columns affected those of panels and vice-versa.

It is worth to note here that the modeling did not consider the size of actual stories in the analysis and in the reading of the results. Another work would focus on this issue.

The model of the analysis was considered in the plane of the wall. The model reflected the geometric shapes of the tested walls. In the analysis, when the number of panels was increased from one panel to two panels or three panels, the increase concerned the height below the lateral displacement control point (shown by a small triangle on each figure) that reflected the shear-span.

For walls C2, C07N10, C07N15 and C10N10, besides the upper actually rigid loading beam at the top of the wall, a rigid beam was assumed at the level of the lateral displacement control point. The vertical steel bars were used as given in the original scheme of the tested walls. As for Walls C07N10, C07N15 and C10N10, the vertical steel bars surrounded by hoops were considered belonging to the columns and when a group of hoops was arranged at the same level (3 hoops), they were considered distributed according to their number.

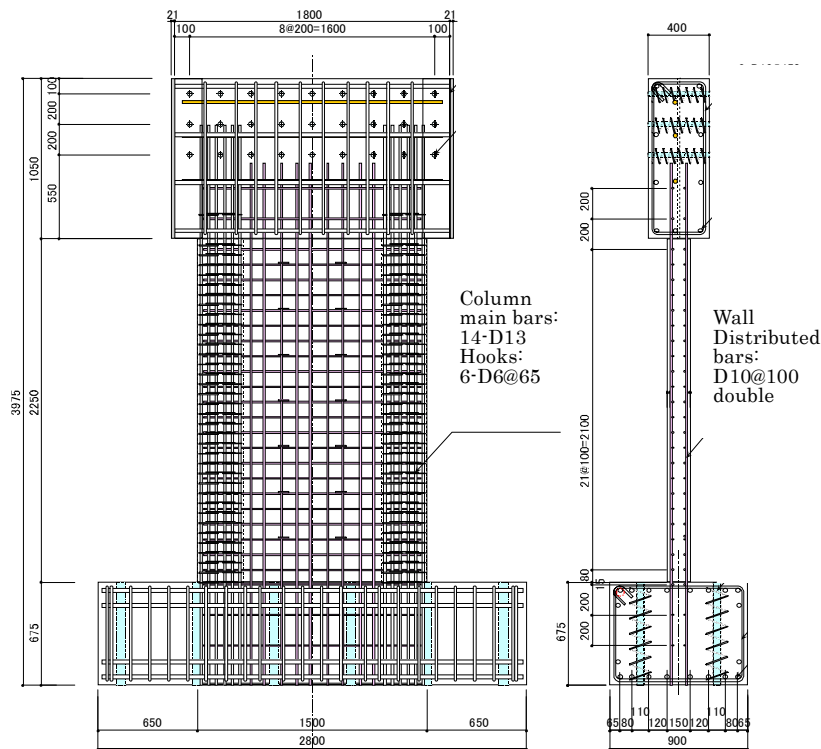


Figure 2 Geometry and detailing: Wall C07N10, Wall C07N15 and Wall C10N10 (Unit: mm)

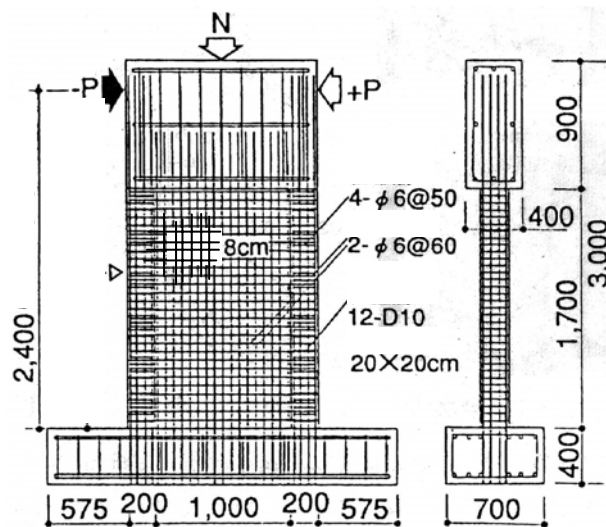


Figure 3 Geometry and detailing: Wall C2 (Unit: mm)

For wall D1, the existing beams at intermediate levels above the displacement control point were modeled as they are.

The member models used in the analysis are the Bilinear hysteresis model for the axial springs (columns and panels), the Degrading Tri-linear hysteresis model for the bending spring (panel) and the Tri-linear hysteresis model for the shear spring (panel). The model envelope curves of all sub-elements are shown in Fig.6 including the main default parameters. The curve characteristics (loading and unloading stiffness, crack and yield levels, etc...) are computed according to the geometry of each element and its material properties

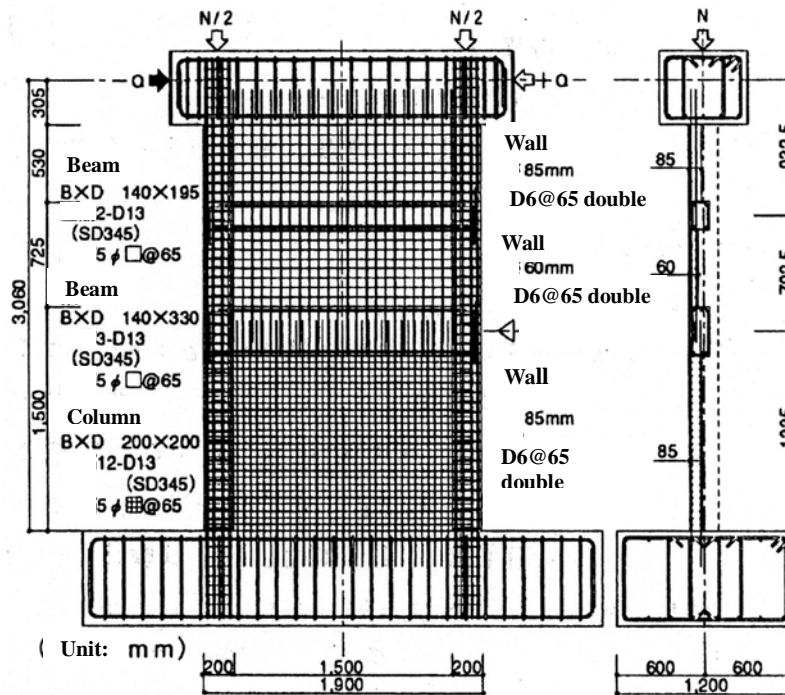


Figure 4 Geometry and detailing: Wall D1 (Unit: mm)

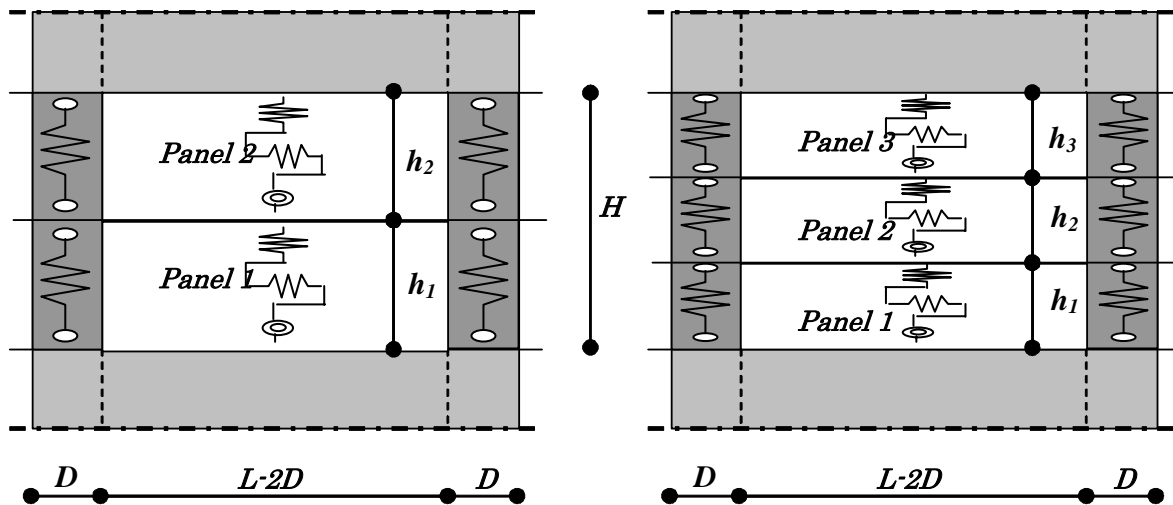


Figure 5 Presumed distribution of panels on the wall height
 (Case of two and three panels)

4. PUSHOVER RESPONSE ANALYSIS OF TESTED WALLS

4.1. Analysis of wall C07N10

This wall was subjected to a constant compression load with an axial load ratio of $\eta = 0.1$ ($N = 1700$ kN) where the concrete strength was equal to 74.9 MPa. By considering, first, the basic parameters (particularly $\phi = 0.9$ and one panel model) constant and equal for all vertical sub-elements constituting the specimen, the system proved to be flexible and the analytical response was relatively far below the experimental curve, as shown in Fig.7. The one panel model (in the figure it was labeled Analysis 1P-0.9 in case of $\phi = 0.9$ and Analysis 1P-0.1 in case of $\phi = 0.1$) did not allow an acceptable matching of

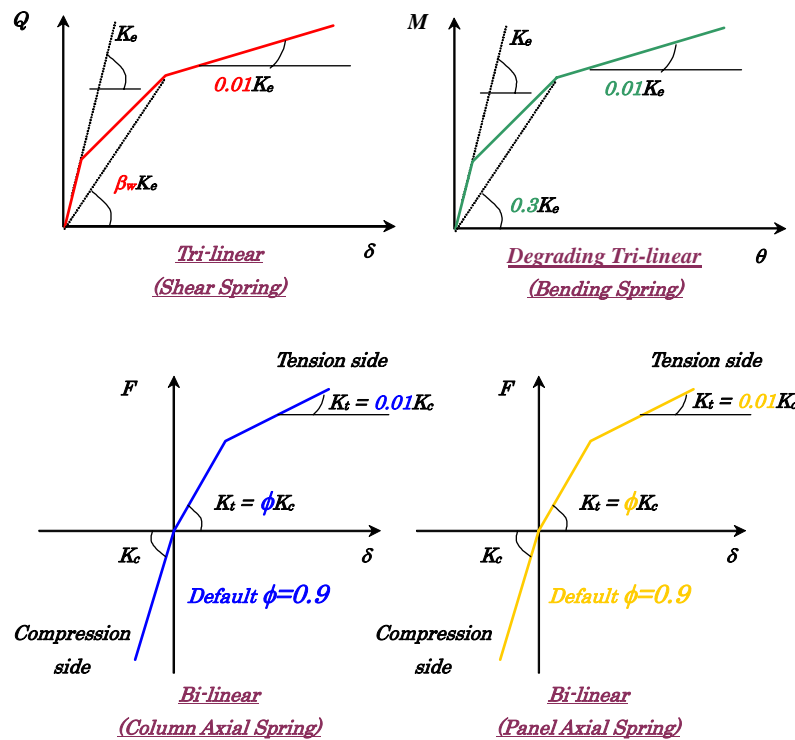


Figure 6 Presumed element models

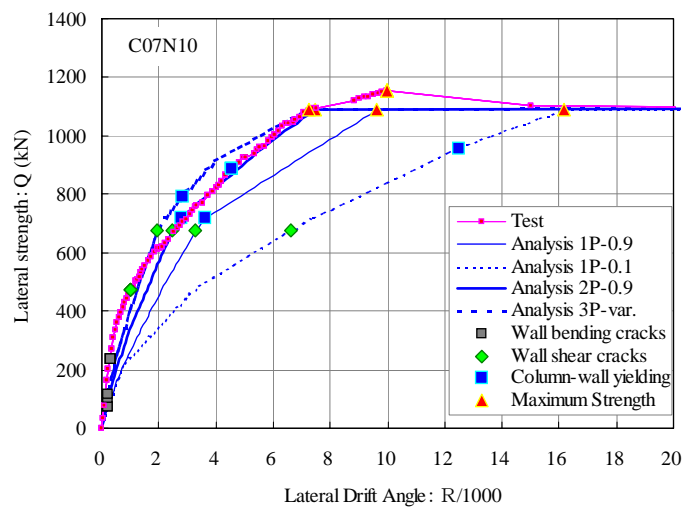


Figure 7 Response simulations of different modeling of wall C07N10

the experimental curve, particularly for the rigidity and also the shear force at intermediate loading levels. However, the maximum shear strength was reached at almost the same lateral drift angle as in the testing for the analysis considering one panel model and $\phi=0.9$. The analysis of more than one panel was then carried out to achieve better results. Trials with two and three panels (in the figure it was labeled Analysis 2P-0.9 in case of two panels and $\phi=0.9$, and Analysis 3P-var. in case of three panels and varying ϕ) were checked (Fig. 7). Although some deficiencies in the evaluation of the lateral drift angle at which flexural cracking, shear cracking and yielding occurred, the experimental curve could acceptably be approached by the analytical curve in two ways:

1. When the part of the wall below the displacement control point modeled by two panels and considering $\phi = 0.9$ for all elements. Such modeling brought the analytical curve very close to the experimental one beyond yielding, however before yielding a gap still existed. Also, the evaluated

maximum shear strength was lower than the test value and occurred at lower lateral displacement.

2. When the part of the wall below the displacement control point modeled by three panels and considering a gradual reduction of ϕ along each element and consequently along the whole height of the wall. The rigidity till the shear cracking of the wall was close to testing results, then the analysis overestimated the response, however such overestimation would be balanced in terms of energy absorption at peak level because the analytical analysis underestimated the maximum strength.

4.2. Analysis of wall C07N15

This wall was under a constant compression load with an axial load ratio of $\eta = 0.15$ ($N = 2500$ kN). The concrete strength was equal to 74.9 MPa. By considering, first, the basic parameters as in Section 4.1, the system proved to be flexible and the analytical response was far below the experimental curve, as shown in Fig.8. The one panel model did not allow an acceptable matching of the experimental curve, particularly for the rigidity and also the shear force at intermediate loading levels. Furthermore, the maximum shear strength was reached at a lateral drift angle before the obtained level in the testing. The analysis of more than one panel was then carried out to achieve better results. Trials with two and three panels were checked (Fig. 8). Although some deficiencies in the evaluation of the lateral drift angle at which flexural cracking, shear cracking and yielding occurred, the experimental curve could relatively be approached by the analytical curve in two ways:

1. When the part of the wall below the displacement control point modeled by two panels and considering $\phi = 0.9$ for all elements. The introduction of two panels shortened the stage at which ultimate conditions occurred and made the system more rigid but the response was still slightly below the testing results during the whole loading process.

2. When the part of the wall below the displacement control point modeled by three panels and considering a gradual reduction of ϕ along each element and consequently along the whole height of the wall. The introduction of three panels without reduction in the tension stiffness ratios (not shown in the figure) shortened more the stage at which ultimate conditions occurred and made the system particularly more rigid for the phase before shear cracking where the analytical response became closer to the experimental curve. Compared to the case without reduction of the tension axial stiffness ratios, the reduction in the tension axial stiffness ratios softened the rigidity beyond shear cracking and increased the deformation at ultimate stage, as presented in the figure.

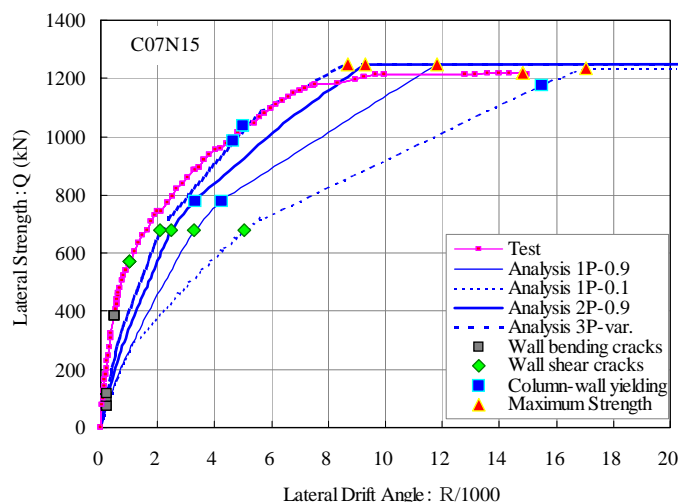


Figure 8 Response simulations of different modeling of wall C07N15

4.3. Analysis of wall C10N10

This wall was subjected to a constant compression load with an axial load ratio $\eta = 0.10$ ($N = 2500$ kN). The concrete strength was equal to 109.1 MPa. Similar observations as in Section 4.1 were drawn for this wall. Although some deficiencies in the evaluation of the lateral drift angle at which

flexural cracking, shear cracking and yielding occurred, the experimental curve could acceptably be approached by the analytical curve in two ways:

1. When the part of the wall below the displacement control point modeled by two panels and considering $\phi = 0.9$ for all elements. The introduction of two panels shortened the stage at which ultimate conditions occurred and made the system more rigid. A good matching with testing was observed beyond yield level.
2. When the part of the wall below the displacement control point modeled by three panels and considering a gradual reduction of ϕ along each element and consequently along the whole height of the wall. Reducing the tension stiffness ratios for both columns and panels seemed more appropriate where the analytical curve approached better the experimental curve, though some gaps that may be equilibrated by the total energy absorption.

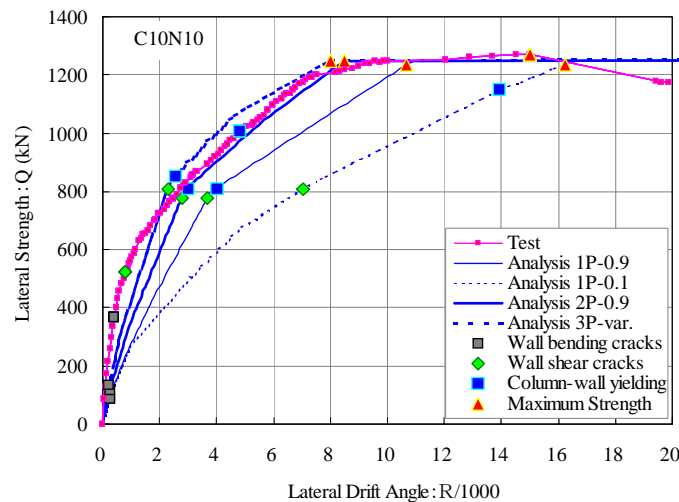


Figure 9 Response simulations of different modeling of wall C10N10

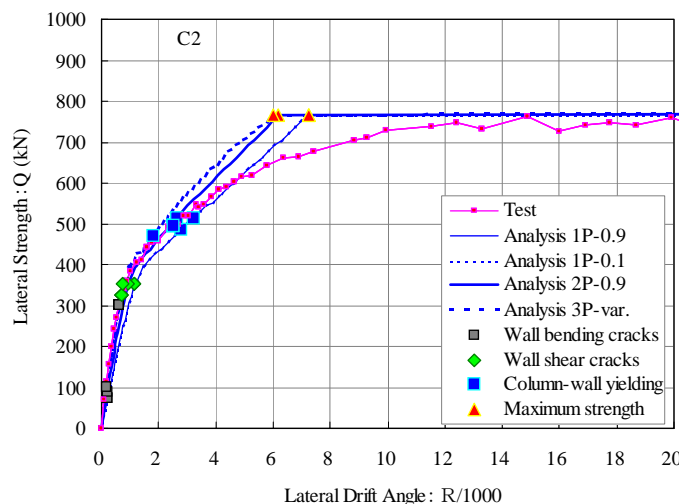


Figure 10 Response simulations of different modeling of wall C2

4.4. Analysis of wall C2

This wall experienced a constant compression load with an axial load ratio $\eta = 0.13$ ($N = 1250$ kN). The concrete strength was equal to 79.0 MPa. When the basic parameters were considered, the system proved to be very slightly flexible and the analytical response was not far from the experimental curve particularly before reaching yield level, as shown in Fig.10. Actually, the response of the one

panel model when $\phi=0.9$ was similar to the response when $\phi=0.1$, which means that the axial stiffness ratio did not affect so much the response. This fact might be due to the column-wall section ratio of this specimen when compared to other specimens. Furthermore, the maximum shear strength was reached at a lateral drift angle far before the obtained level in the testing. The analysis of more than one panel was then carried out to achieve better results. Trials with two and three panels were checked and proved to be effective but without any effect of the tension axial stiffness ratio (Fig. 10). Although a certain gap beyond yielding, the experimental curve could acceptably be approached by the analytical curve in two ways:

1. When the part of the wall below the displacement control point modeled by two panels and considering $\phi = 0.1$ for all elements. Therefore, the response was also very close to the case when $\phi = 0.9$ that was shown in the figure.
2. When the part of the wall below the displacement control point modeled by three panels and considering a gradual reduction of ϕ along each element and consequently along the whole height of the wall. Actually, for this case also, the response with gradual change was almost similar to the case of $\phi=0.1$ and $\phi=0.9$ for the same three-panel model.

4.5. Analysis of wall D1

This wall was under a constant compression load with an axial load ratio $\eta= 0.11$ ($N = 1350$ kN). The concrete strength was equal to 63.0 MPa. Similar observations as in Section 4.1 were drawn using the basic parameters, as shown in Fig.11. Furthermore, the maximum shear strength was higher and reached at a lateral drift angle far before the obtained level in the testing. The analysis of more than one panel was then carried out to achieve better results. Trials with two and three panels were checked (Fig. 11). Although a small gap beyond maximum strength and some differences in the level at which bending cracks or yielding occurred, the experimental curve could acceptably be approached by the analytical curve in two ways:

1. When the part of the wall below the displacement control point modeled by two panels and considering $\phi = 0.9$ for all elements. Except the maximum strength, this model brought the response very close to the testing results.
2. When the part of the wall below the displacement control point modeled by three panels and considering a gradual reduction of ϕ along each element and consequently along the whole height of the wall. For this case, the gradual change reduced slightly the stiffness beyond shear cracking and had almost an average response between the case of $\phi=0.1$ and $\phi=0.9$ for the same three-panel model.

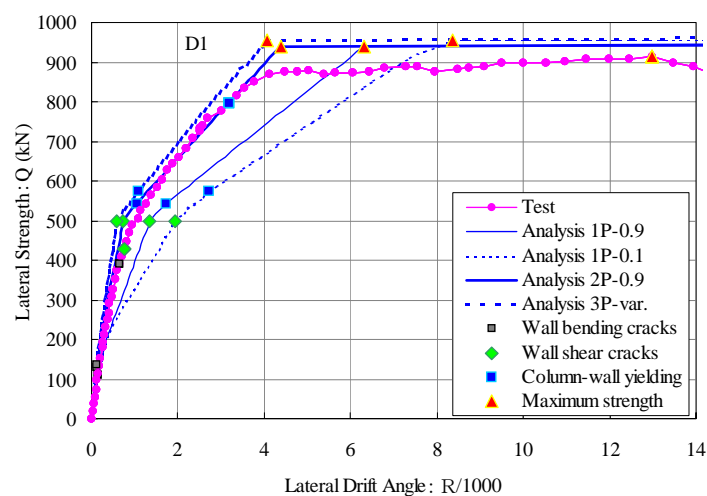


Figure 11 Response simulations of different modeling of wall D1

5. DISTRIBUTION OF TENSION AXIAL STIFFNESS RATIO

From the simulations carried out on different modeling of the five specimens, it was found that the one panel model, considering the original tension axial stiffness ratio of 0.9, was relatively flexible when compared to test results. The presumed two-panel and three-panel models could bring the analytical response close to the testing results. The tension axial stiffness ratios varied according to the modeling. From the selected cases shown in the previous sections, a preference for the value of the tension stiffness ratio that brought the analytical response very close to the test results is illustrated in Table 2.

While the values for the two-panel model were constant and equal on the height of the wall sub-elements (columns and panels) thus simple to apply without any difficulty, the values for the three-panel model appeared more realistic with their gradual change on the height of the sub-elements and their different assigned values for columns and panels.

Table 2 Distribution of the average tension axial stiffness ratio

Model	Wall Level	C07N10		C07N15		C10N10		C2		D1	
		C	P	C	P	C	P	C	P	C	P
Two Panels	Upper panel	0.9	0.9	0.9	0.9	0.9	0.9	0.9*	0.9*	0.9	0.9
	Lower panel	0.9	0.9	0.9	0.9	0.9	0.9	0.9*	0.9*	0.9	0.9
Three Panels	Upper panel	0.75	0.225	0.55	0.225	0.75	0.225	0.60*	0.225*	0.60	0.225
	Central panel	0.65	0.175	0.45	0.175	0.65	0.175	0.40*	0.175*	0.40	0.175
	Lower panel	0.55	0.125	0.35	0.125	0.55	0.125	0.20*	0.125*	0.20	0.125

Notes: C = Column, P = Panel, The average tension axial stiffness ratio means the average of ratios at the bottom and top of a sub-element below the wall's displacement control point, * = values selected subjectively and made similar to other specimens' values as long as ratios 0.9 or 0.1 or in between induced for this case very similar responses where all matched experimental results

For the two panel case of modeling, the values of the tension stiffness ratio obtained from the analysis of the wall C2 were opposing the withdrawn general conclusion, where an actual value of 0.1 was obtained instead of the general value of 0.9 as for other wall-specimens. Actually, when selecting the value 0.9 for wall C2, the response was very close the response when the value 0.1 was selected and the changes from one extreme case to another one did not affect very much the response, except in the delay of the ultimate and yielding stages. This fact might be explained by the following: while all columns in other specimens have almost the same column-wall cross-section ratios, wall C2 was different, as it is shown in Table 1. The very high section size proportion of the columns compared to the section size of the panel was suspected to be the reason of the relatively slight difference of the response when both extreme values of the tension stiffness ratio are selected.

As for the case of three-panel model, while the assigned values for panels were the same for the panels of walls with rectangular shape or with boundary columns, except when the axial load ratio was high, those for columns were different where the variation was softer in the case of walls with rectangular shape besides the effect of the axial load ratio (Table 2). For both type of walls, the gradual step for panels was 0.05 with an initial value of 0.125 at the lowest level. As to the ratios of columns, the applied axial load ratio affected the values of the tension axial stiffness but did not affect the gradual step distribution through the height of the wall. A higher axial load ratio induced lower tension axial stiffness ratios, as in the case of panel C07N15. For walls with boundary columns, the gradual step for boundary columns was 0.2 with an initial value of 0.2 at the lowest level. For walls with rectangular shape, the gradual step for columns was 0.1 with an initial value of 0.55 at the lowest level for low axial load ratios and 0.35 for high axial load ratios.

6. CONCLUSIONS

The result of various trials, simulations and comparisons of pushover response analyses to test results of five reinforced concrete wall specimens of different shapes (walls of rectangular shape or with boundary columns) made of high-strength materials were summarized in this study. For each tested specimen, comparisons were made as to the basic analytical case of the original model proposed by Kabeyasawa. The following comments and conclusions were intended for reinforced concrete walls similar to the walls presented in this study:

1. The basic analytical model, generally, brought satisfaction as to the evaluation of the maximum shear strength however it underestimated the response in terms of energy absorption, according to the characteristics of the walls, particularly for walls of rectangular shape.
2. Modeling the wall by just one panel reached acceptable results in terms of shear strength, but it seemed underestimating the rigidity before yielding of the system. In other terms, the wall seemed to be more flexible than in the test case.
3. Increasing the number of panels brought the analytical curve very close to the experimental one. Two-panel-modeling generally achieved better matching beyond yielding of the system and underestimated the part before yielding where the lack was in the rigidity. Three-panel-modeling achieved better matching before yielding of the system and overestimated the part after yielding.
4. Varying the tension stiffness ratios of the sub-elements in a wall system was a complicated task. Changing the ratios of the columns would affect those of the panels and vice-versa. Thus, the variation would result in the following:
 - i. Higher values of ϕ achieved better results in terms of force and rigidity for all types of walls.
 - ii. Lower values of ϕ achieved better results in terms of deformation for the case of walls of rectangular shape, however for walls with boundary columns the variation did not affect significantly the response.
 - iii. Low values of ϕ for panels, in combination to those of columns, delayed the ultimate stage for the case of walls of rectangular shape, however for walls with boundary columns the variation seemed affecting slightly the response.
 - iv. Low values of ϕ for columns, in combination to those of panels, for both types of walls delayed the yield stage.
5. When more than one panel was considered in the modeling, varying the tension stiffness ratios ϕ along the height of the wall brought better results, however, exact values were very difficult to achieve. For a given element, being column or panel, the bottom part should be given lower ϕ value than its upper part.
6. By reference to the limited data, the two-panel modeling with a constant ratio $\phi=0.9$ would be simple for application, though some acceptable deficiencies, namely the gap in the rigidity before shear cracking stage. The three-panel modeling would also be advisable, particularly in the phase before shear cracking.
7. For the particular case of high column-panel section ratio, the selection of different values for the tension stiffness ratio might not affect the response as it was found for wall C2 with two-panel modeling, however, to uniform the application a value of 0.9 could be considered.
8. Applied axial load ratio level affected the tension axial stiffness ratios of the columns of the walls of rectangular shape when modeled with three panels, as it was found for wall C07N15. Higher axial load ratio induced lower tension axial stiffness ratios.
9. For convenience, suitable values to be considered when simulating the response of similar walls were suggested for two and three-panel modeling.

REFERENCES

- A.I.J., J.S.C.E. and J.G.S. (2001). Report on the Damage Investigation of the 1999 Kocaeli Earthquake in Turkey. Architecture Institute of Japan.
- Bechtoula, H., Ousalem, H. (2005). The 21 May 2003 Zemmouri (Algeria) earthquake: Damages and disaster responses. *Journal of Advanced Concrete Technology*, Japan Concrete Institute, **3:1**, 161-174.
- Kabeyasawa, T., Shiohara, H., Otani, S., and Aoyama, H. (1983). Analysis of the Full Scale Seven-Story Reinforced Concrete Test Structure. *Journal (B) of the Faculty of Engineering, The University of Tokyo*, **37:2**, 432-478.
- Kabeyasawa, T. and Milev, J.L. (1997). Modeling of Reinforced Concrete Shear Walls under Varying Axial Load. *Transactions of the 14th International Conference on Strcutural Mechanics in reactor Technology (SmiRT 14)*, France.
- Kangning, L., Aoyama, H. and Otani, S. (1988). Reinforced Concrete Columns under Varying Axial Load and Bi-Directional Lateral Load Reversals. *Proceedings of the 9th WCEE, Japan*, 537-544.
- Kangning, L. and Otani, S. (1993). Multi-Spring Model for 3-Dimensional Analysis of RC members. *Journal of Structural Engineering and Mechanics*, **1:1**, 17-30.
- Kimura, H. and Ishikawa, Y. (2006). A Study about the Structural Performance of Earthquake Resistant Reinforced Concrete Shear Walls of Rectangle Cross-Section. *Proceedings of the Conventional Conference of the Japan Concrete Institute, Niigata, Paper No. 2079*, **28:2**, 469-474. (Japanese)
- Ousalem, H., Bechtoula, H. (2003). Report on the damage investigation and post-seismic campaign of the 2003 Zemmouri earthquake in Algeria. Earthquake Research Institute, The University of Tokyo, Ohbunsha Press.
- Takeda, T., Sozen, M.A. and Nielsen, A.A. (1970). Reinforced Concrete Response to Simulated Earthquakes. *Journal of Structural Division, ASCE*, **96:ST12**, 2557-2573.
- Takenaka Research and Development Institute (2003). Examination on the Analysis and Modeling of Aseismic Shear Walls. Internal Report of Takenaka Research and Development Institute. (Japanese)
- Vulcano, A. and Bertero, V.V. (1986). Analytical Models for Predicting the Lateral response of RC Shear Walls: Evaluation of their Reliability. UCB/EERC Report No. 87/19.